Towards Deep Learning Based Estimation of Fracture Risk in Osteoporosis Patients

Costin Florian Ciuşdel[*,†], Anamaria Vizitiu[*,†], Florin Moldoveanu[†], Constantin Suciu[*,†], Lucian Mihai Itu[*,†]
[*] Corporate Technology, Siemens SRL, Brasov, Romania
[†] Department of Automation and Information Technology, Transilvania University of Brasov, Brasov, Romania

***Abstract*—Osteoporosis is a skeletal disorder which leads to bone mass loss and to an increased fracture risk. Recently, physics-based models, employing finite element analysis (FEA), have shown great promise in being able to non-invasively estimate biomechanical quantities of interest in the context of osteoporosis. However, these models have high computational demand, limiting their clinical adoption. In this manuscript, we present a deep learning model based on a convolutional neural network (CNN) for predicting average strain as an alternative to physics-based approaches. The model is trained on a large database of synthetically generated cancellous bone anatomies, where the target values are computed using the physics-based FEA model. The performance of the trained model was assessed by comparing the predictions against physics-based computations on a separate test data set. Correlation between deep learning and physics-based predictions was very good (0.895, $p < 0.001$), and no systematic bias was found in Bland-Altman analysis. The CNN model also performed better than the previously introduced Support Vector Machine (SVM) model which relied on handcrafted features (correlation 0.847, $p < 0.001$). Compared to the physics based computation, average execution time was reduced by more than 1000 times, leading to real-time assessment of average strain. Average execution time went down from 32.1 ± 3.0 seconds for the FE model to around 0.03 ± 0.005 seconds for the CNN model on a workstation equipped with 3.0 GHz Intel i7 2-core processor.**

Keywords—convolutional neural network; osteoporosis; prediction; simulation; trabecular.

I. INTRODUCTION

Osteoporosis is a skeletal disorder which leads to bone mass loss and diminished bone strength (as characterized by density and quality), and, hence, to an increased fracture risk. Bone loss typically appears due to a deficiency of estrogen in postmenopausal women, or due to other age related mechanisms (e.g. secondary hyperparathyroidism, reduced mechanical loading, etc.) [1].

Since effective drug therapies are available, it is crucial to correctly diagnose the onset of osteoporosis so as to minimize the future risk of fractures.

A total of 3.7 million osteoporotic fractures were estimated in 2000, whereas approx. 24% represented hip fractures. Crucially, healthcare costs were estimated at a level of €36.2 billion, whereas hip fractures caused two-thirds of the expenses.

Furthermore, osteoporosis related healthcare costs are expected to more than double to around €76 billion by 2050 [2], since the estimated number of hip fractures alone is expected to increase to 6.3 million by 2050 [1]. According to the International Osteoporosis Foundation, osteoporosis affects approximately 75 million people in Europe, USA and Japan. One in three women over 50 will experience osteoporotic fractures, as will one in five men. In women over 45 years of age, osteoporosis accounts for more days spent in hospital than any other disease, including diabetes, myocardial infarction and breast cancer.

A. The Human Bone

Bone is a living material which can regenerate. Its structure and density adapt as a result of the mechanical forces acting on it [3]. Specifically, the bone architecture is optimized so as to resist forces with the smallest possible amount of material.

Two important characteristics describing bone mechanics under loading conditions are:

1) Strain: deformation of the bone in relation to its initial state.

2) Stress: internal forces of the bone.

Depending on the values of these two quantities, the bone is in the pre-yield, post-yield, or ultimate state (Fig. 1). In the pre-yield state, deformations are purely elastic, i.e. any deformation is temporary and the initial state of the bone is recovered once the load disappears. The most relevant material property for the pre-yield state is the Young's modulus (stiffness or modulus of elasticity). It is the slope of the stress-strain curve, and represents the pressure which is required to act upon a bone to obtain a certain deformation. Once the yield point is surpassed, the deformation becomes plastic, and, thus, permanent.

The yield point is characterized by the yield strain, the yield stress and the yield strength. Alternatively, bone toughness is used, representing the total energy which the bone can absorb before it passes the yield point. The ultimate state is described by the ultimate strain, the ultimate stress and the ultimate strength.

Bone material is encountered in the human body either as cortical / compact bone or as cancellous / trabecular bone. On average, 80% of the bone mass is cortical and these regions of the bone ensure its stability. Cancellous bone typically resides inside of a frame formed of cortical bone and has a sponge

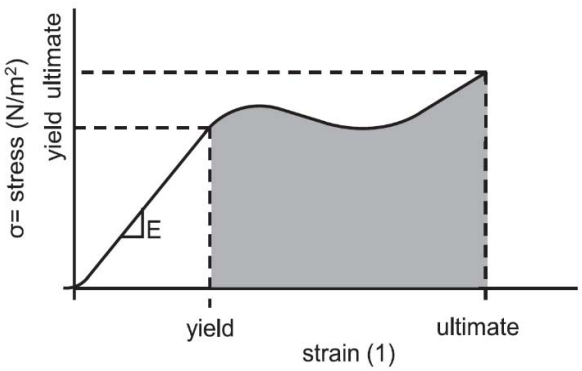

Fig. 1. Smoothened stress-strain curve. White: pre-yield; gray: post-yield; transition: yield point; ultimate yield: fracture. E: Young's modulus based on slope of stress–strain curve [3].

like appearance. Its density is much smaller than that of cancellous bone.

B. Previous Work

Research studies conducted during the last decades and more intensively during the last years have shown that biomechanical modeling techniques, based on finite element analysis (FEA), bear great potential for improving clinical decision making processes [4]. These techniques combine geometrical information extracted from medical imaging (structural properties, anatomical shape) with background knowledge on the patient (e.g. demographics) and patient-specific information (e.g. loads), encoded in a complex mathematical solid mechanics model consisting of partial differential equations which can be solved only numerically. This approach leads to a large number of algebraic equations, making it computationally very demanding. Typically, the solution of these models requires a time frame from a few minutes to a few hours for high-fidelity models representing the complete three dimensional space. Since the FEA analysis is typically based on CT (computed tomography) imaging data, it is sometimes also called biomechanical CT (BCT).

One alternative proposed in literature is 3D statistical shape and appearance modeling [5]. It employs a database of 3D bone images and is based on the average shape and density distribution and their main modes of variation. To determine the shape and density of a patient-specific bone, only the contributions of the main modes to the shape and distribution of the current bone need to be determined. Thus, a 2D image, as acquired through DXA (dual-energy X-ray absorptiometry), may be used, followed by a 2D - 3D matching algorithm which outputs the weights of the contributions. This methodology circumvents the usage of QCT (quantitative CT) and image segmentation. A FEA may be performed based on the resulting 3D model.

Recently, a methodology based on machine learning was employed to predict measures of interest extracted from FEA (i.e. stress) [6]. A database of 89 femur bones was used, and features were based on a statistical shape model, and morphometric and density information. The distribution of stress was predicted with a correlation of 0.98.

Previously, we have introduced a machine learning model (SVM – Support Vector Machine) based on features extracted from 3D anatomical models of cancellous bone segments [7]. Eleven different handcrafted features were generated, reflecting the voxel connectivity in the cancellous structure.

In this paper, we present a deep learning (DL) model for computation of trabecular bone biomechanics, as an alternative to FEA-based modeling, and show that the performance of the model is statistically very similar to that of the FEA approach. Furthermore, we compare the results against the SVM based results obtained. The DL model is trained and evaluated using a synthetically generated database of 25000 trabecular bone anatomies, resulting in a rich sampling of the different morphologies of these anatomies.

As described before [7], a FEA model is used to compute the strains and stresses for each trabecular bone anatomical model. Subsequently, we determine the average strain for each geometry. A deep learning model is then trained to learn the relationship between the anatomical model and the strain computed using the FEA model. Once the model is trained, the computational time for predicting the strain value for a new case is significantly lower than that of the FEA model, going from 32.1 ± 3.0 seconds for the FEA model to approx. 0.03 seconds for the DL model on a standard desktop computer (workstation equipped with a 3.0 GHz Intel i7 2-core processor).

In the rest of the paper, we distinguish between the strain computed with the FEA model (ϵ_{FEA}) and with the deep learning model, i.e. convolutional neural network (ϵ_{CNN}).

II. Methods

A. Overall Workflow

The deep-learning based model proposed herein is trained offline on a large database of synthetically generated cancellous bone anatomies. The prediction phase is an online process, whereby the algorithm computes ϵ_{CNN} for a given patient's data, by using the learned mapping from the training phase. Given an anatomical bone model, the computation of ϵ_{CNN} is fully automatic, without requiring user intervention. The pre-processing pipeline required to generate the anatomical model can also be fully automated. A single ϵ_{CNN} value is computed for the entire model (the average strain). A schematic of the workflow is shown in Fig. 2.

A typical approach for generating a patient-specific bone anatomical model is to employ a medical imaging device, such as micro-CT (computed tomography), for acquiring images of the tissues of interest. A 3D cancellous bone anatomical model can be reconstructed from these images to reflect the shape and structure of real tissues (Fig. 3). Such a model typically consists of a 3D binary matrix, where a value of "1" denotes the presence of a bone voxel and a value of "0" denotes a gap. In the absence of patient-specific data, we employ synthetically generated data for the validation of the DL model.

The anatomical model is fed to a 3D convolutional neural network, which outputs the global average strain. Based on the

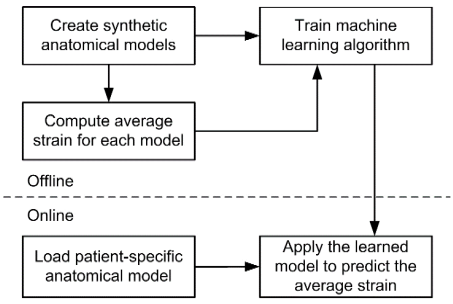

Fig. 2. Overall workflow of the proposed framework.

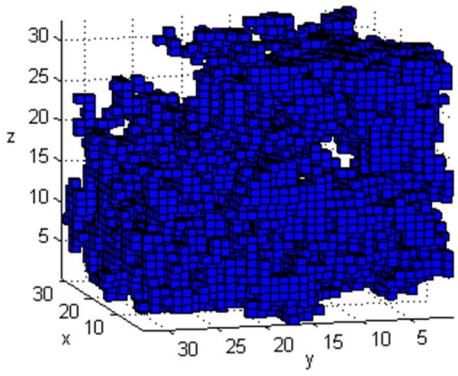

Fig. 3. 3D anatomical model of a cancellous bone segment.

predicted value, further calculations can be conducted to determine the fracture risk in percentage.

B. *Generation of Synthetic Training Database*

To train a prediction model, a dataset containing a large number of training examples is required. Such a dataset is difficult to generate from patient-specific data, since it requires an extensive number of patient records. Herein we resort to a synthetic database which has multiple benefits:

1) The entries can be created *in silico* with specific desired properties such as density / sparsity.

2) There is no obvious limit on the number of examples that can be generated.

3) Complex pathological configurations can be generated.

4) Rare pathological cases can be sampled better.

5) Since the generation of synthetic *in silico* geometries can be completely automated, the cost of generating a large database is reduced.

6) The methodology can be extended to different demographic groups.

7) The training can be performed in a global or in a site-specific manner. This allows the system to account for anatomical trends based on patient demographics and epidemiology.

8) The training can be iteratively improved with more data.

To generate synthetic data of the type depicted in Fig. 3, we employ the following workflow:

1) The size of the domain (number of voxels in each direction) is set to 32x32x32.

2) A 3D matrix of the chosen size of uniformly distributed random numbers in the range of (0, 1) is generated. A varying threshold for classifying the voxels into bone voxels or empty voxels is chosen (e.g. between 0.63 and 0.67).

3) A filter is applied to remove all but the largest island of the matrix, and also to discard any poorly connected voxels.

4) Post-processing is performed to improve the statistical properties of the structures so as to resemble patient-specific cancellous data. Specifically, the post processing algorithm searches for certain types of gaps in the voxel structure and fills them. For example, if two voxels on the same line / column are separated by a gap, the corresponding voxel is turned into a bone voxel. This algorithm is applied at slice level for various plane orientations (i.e. parallel to the xOy, xOz, yOz planes). The post-processing step improves the voxel connectivity, having a positive effect on the structural robustness. Fig. 4 displays an example of a slice of the 3D matrix, before and after post-processing.

A synthetic dataset consisting of 25000 anatomical models was generated. Each geometry was meshed and a FEA was conducted. Each "1" in the binary matrix was meshed as a cube of side length equal to 0.15936 mm (Young's modulus was set to 17 GPa and Poisson's ratio to 0.3 [8]). An in-house developed FE solver was used, based on [9] as reference. The structural analysis problem formulation was based on the principle of virtual displacements:

$$\int_V \bar{\epsilon}^T \tau \, dV = \int_V \overline{U}^T f^B dV + \int_{S_f} \overline{U}^{S_f^T} f^{S_f} \, dS + \sum_i \overline{U}^{iT} R_C^i \qquad (1)$$

This principle states that energy contained in an elastic body after a deformation is equal to the sum of virtual work of volume, surface and point-wise forces acting on the body. By discretizing the above integrals, a large system of linear equations was derived, whereas the unknown values were the nodal displacements.

The FE solver performed static linear analyses using 8-node quadrilateral finite elements. Its output precision was tested and validated against the Ansys Mechanical FE analysis suite.

The following boundary conditions were applied for the FEA:

1) The bottom layer of nodes was fully constrained.

2) The combined load on the Oz axis for the top layer of nodes was computed so that the whole structure would support a prescribed weight. This weight was derived from an organ level simulation of a femur (Fig. 5): a femur (modeled as an isotropic material) was loaded with 90 kg using boundary conditions described in [10]. A slice was selected as visualized in fig. 5 (in the femoral neck) and the corresponding stress 'S' was noted. The prescribed weight used for the cancellous FEM simulation was computed by multiplying 'S' with the area of a 32 by 32 slice of voxels.

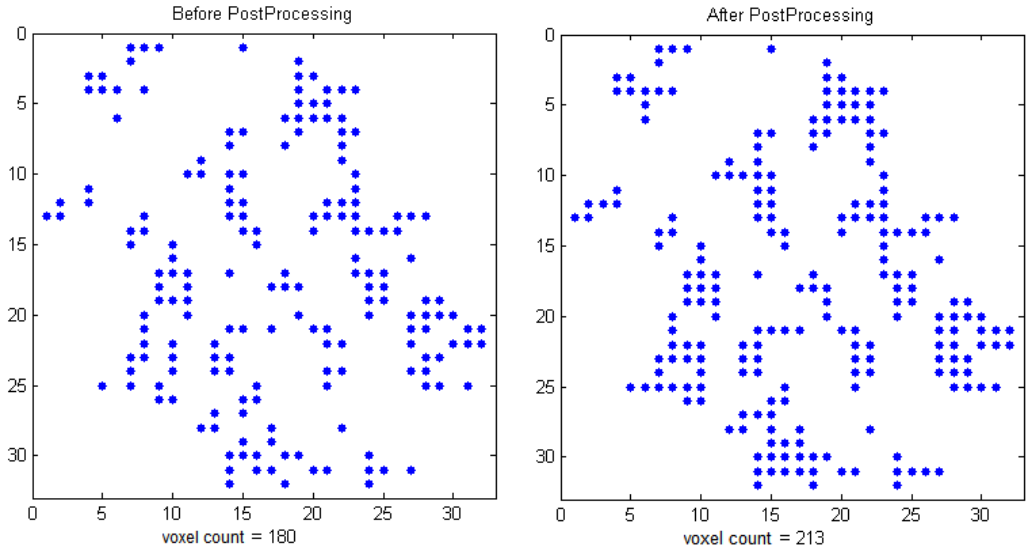

Fig. 4. 2D slice of synthetic data before and after applying the post-processing algorithm.

The average (normal) strain was computed over all the finite elements. The 3D binary matrix together with the computed average strain of each geometry represented an entry in the training dataset of the DL model. Furthermore, each geometry was rotated by 90˚ around the Oz axis (the same average strain is obtained since the geometry itself is not altered). The resulting datasets were also added to the training database, leading to a total number of 50000 training datasets. This augmented dataset allowed the prediction model to become invariant to the Oz angular position of the analyzed structure in the base coordinate system.

Similarly, a separate test dataset was created, comprising 4000 samples, which was used for the evaluation of the trained DL model.

C. Convolutional Neural Network

A 3D convolutional neural network (CNN) was used to learn the dependence between the anatomical model and the resulting global strain for the loading scenario described above. The anatomical model served as the input volume of the network. Convolutional filters were applied sequentially, reducing the volume size and thus creating localized features, and two final, fully connected layers of neurons computed the output value. Each layer used leaky-ReLU (rectified linear unit) as activation functions, with negative slope equal to 0.01.

The network architecture is presented in Fig. 6. First, 32 2x2x2 3D filters were applied with stride 2 in all directions, resulting in a volume of size 16x16x16 with 32 channels. Secondly, 64 2x2x2 filters were applied with stride 2 in all directions resulting in a reduced 8x8x8 volume with 64 channels. One possible interpretation of the effect of these filters is that they search for microstructures in the input volume. Each entry in the second 8x8x8 volume represents a 4x4x4 sub-volume of the original input. These microstructures can be further combined / analyzed so as to obtain a global measure of structural rigidity, e. g. strain.

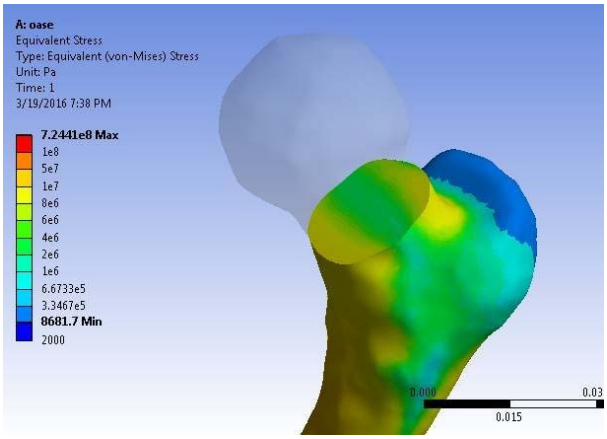

Fig. 5. Stress results obtained after performing an organ level loading simulation for a human femur bone.

Thirdly, 128 2x2x2 filters with stride 1 were applied, resulting in a 7x7x7 volume with 128 channels. Fourthly, 8 1x1x1 filters with stride 1 were applied, resulting in a 8-channel volume with the same 3D dimensions. These last 8 filters were used to reduce the number of channels of the resulting localized feature volume. A fully connected layer comprising 64 neurons was used on this volume. The final output layer consisted of only one neuron which computed the predicted strain value by employing a linear combination of the activations of the 64 neurons of the previous layer.

Overall, four convolution layers and two fully connected layers were employed. The resulting model comprised approximately 260000 parameters. Training was conducted using the 3D Caffe framework [11]. Stochastic gradient descent was used with a momentum value equal to 0.5. The weight decay value was set to 0.0075. The base learning rate was 0.001, being step wise decreased. Training consisted in 150 epochs, i.e. passing through all the training dataset 150 times. These optimal hyper-parameter values were chosen

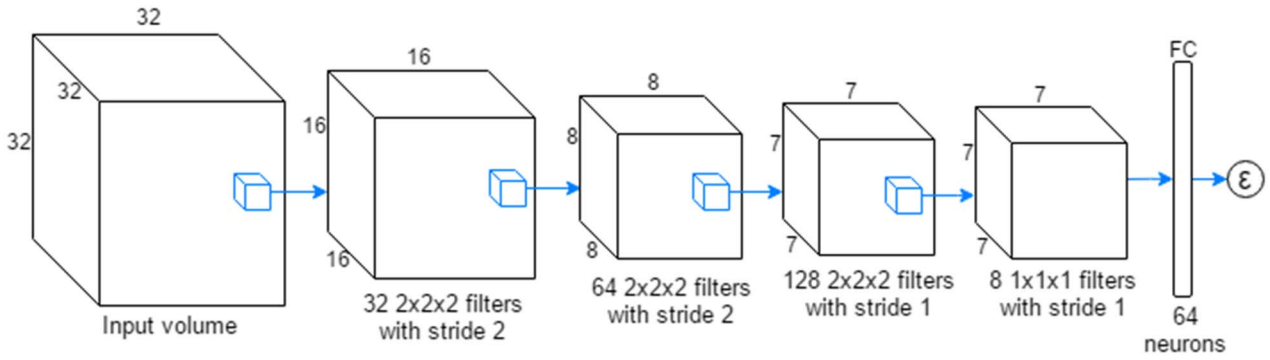

Fig. 6. The convolutional neural network architecture

following a grid search procedure. The employed loss function was the minimization of the square Euclidean distance between the predicted value and the target strain value. Final loss values were 1.5e-3 for the training dataset and 3.6e-3 for the test dataset, suggesting a marginal overfit.

Since the computed strains were in the order of 10^{-3}, the strains in the test and train datasets were normalized to the range (0, 1), to avoid numerical precision issues.

III. RESULTS

We first validated the FEA solver against the Ansys Mechanical FE analysis suite, by running simulations with a bone tissue cube which discretized in a 32x32x32 grid of 8-node quadrilateral elements (of size 0,16mm) consisting of 35937 nodes. A -0,017mm displacement on the Oz axis was enforced for the top layer of nodes, and the nodes in the bottom layer were fully constrained. The resulting nodal displacements were compared against those obtained with Ansys. For the Ox and Oy axes (perpendicular to the loading axis) the mean absolute relative error was 0.1% and the maximum absolute relative error was 6.2%. For the Oz axis, the mean absolute relative error was 0.07% and the maximum absolute relative error was 5.7%.

Next, we evaluated the CNN approach on the test data set consisting of 4000 samples. Prediction accuracy was evaluated as follows. For each predicted strain value, an absolute relative error was computed as:

$$e_{rel} = \frac{|\epsilon_{FEA} - \epsilon_{CNN}|}{\epsilon_{FEA}} \quad (2)$$

The average relative error was subtracted from 1 and the result was multiplied by 100 to obtain the final accuracy score in percentage. The results obtained with the convolutional neural network were compared with those obtained with SVM, which is based on handcrafted features (on the same training dataset), as described in [7].

The total prediction accuracy was 93.8% for CNN and 93.0% for SVM. The correlation (Pearson's product-moment coefficient) between ground-truth and CNN prediction was 0.895. For SVM, the correlation was 0.847.

The average execution time went down from 32.1 ± 3.0 seconds for the FE model to around 0.03 ± 0.005 seconds for the CNN model on a workstation equipped with 3.0 GHz Intel i7 2-core processor.

Both prediction models were invariant to the orientation of the analyzed structure on the Oz axis (the axis the load was applied on). The mean ± SD difference between the prediction values for the same structure under different orientations was -5.6e-5 ± 3.4e-3 for CNN. Compared to the entire range of normalized target strains (0, 1), these difference values indicate that the CNN prediction model is symmetric with respect to the Oz axis, i.e. the predicted values are invariant with respect to the structure orientation.

Fig. 7a and 7b display the histograms of the normalized strains in the test and training datasets respectively: most of the samples are in the lower part of the normalized spectrum, while few samples have larger values.

Fig. 8 depicts a scatter plot of the results on the test set, for both the CNN model and the SVM model. Table 1 presents a detailed view of the distribution of prediction errors for various strain ranges. Errors are small for low strains and increase for larger values of strain, an aspect which is mainly caused by the fact that the majority of training samples are high density low-strain structures. Accuracy for larger-strain entries can be improved by adding more structurally sparse geometries in the synthetic dataset. The CNN lead to a better generalization when compared to SVM, i.e. it had better prediction accuracy for sparser geometries (of larger strain).

Fig. 9 displays a Bland-Altman analysis for $\epsilon_{CNN/SVM}$ vs. ϵ_{FEA}. The mean ± SD difference between the FE computed strains and the CNN predicted ones was 1.7e-3 ± 0.04, indicating that the CNN model did not produce any bias. The CNN model also lead to narrower agreement limits compared to the SVM model.

The receiver-operator characteristic (ROC) curve is shown in Fig. 10. To generate the ROC curve, varying threshold values were applied for the computed strains (FEA and CNN/SVM), to discriminate between fracture / non-fracture conditions: strains above the threshold value were considered to be indicative of fractures. The area under curve (AUC) of the ROC plot was 0.964 for CNN and 0.956 for SVM, suggesting that the CNN had better classification capabilities than the SVM.

IV. Discussion

We have introduced a deep learning based algorithm for a real-time computation of average strains from cancellous bone anatomical models. Our approach is potentially well-suited for a clinical setting since it is computationally efficient both in terms of execution speed and hardware requirements.

The above described results suggest that the proposed CNN architecture can learn the mechanical characteristics, e.g. structural rigidity, of anatomical trabecular structures. Specifically, no handcrafted features are required: the CNN model in Fig. 6 automatically learns higher order features representative for the computed strain. This is in contrast with the previously introduced SVM based model which relied on handcrafted features.

The key ingredients for the design of our deep learning method are the availability of a comprehensive database of training data. In an ideal scenario, the training database would consist of thousands of patient-specific anatomical models extracted from medical imaging data, accounting for the variability of trabecular structures across different patient populations. From a practical point-of-view, establishing such a large database would be prohibitively expensive and time-consuming.

To address this issue, we introduced the concept of a training database consisting of synthetically generated cancellous bone geometries, and corresponding strain values computed from a FEA algorithm. After training, the deep learning algorithm encodes the correlation between the trabecular structure model and the quantity of interest, herein average strain predicted by the validated FEA model.

Our approach can also be extended to compute other quantities of interest, such as whole-bone strength, load-to-strength ratio, local/average stress, local strain or local/global stiffness, each of which can be used as a ground-truth in the training database.

It should be noted that the presented approach is generic with respect to the FEA model used for training the algorithm. For this work, we employed static linear analyses. On the other hand, our results also point to the fact that the accuracy of ϵ_{CNN} will depend on the accuracy of ϵ_{FEA} used in the training phase. In general terms, the performance of our method is expected to be statistically similar to that of the FEA model.

Since a linear finite element analysis was employed for generating ground truth data, if the load is increased by a certain factor, the resulting strain increases by the same factor. Therefore, for a specific load, the final strain value can be computed by scaling the predicted value. Furthermore, if the patient-specific Young's modulus is higher by a factor **c** than the value used in the training dataset, the resulting strain has to be scaled by (1/**c**) to obtain the patient-specific strain value.

The constant **c** can be estimated from the apparent density of the trabecular structure [12]. A linear simulation is valid for the majority of materials for small strains. A specific workflow for estimating patient-specific fracture risks was introduced previously [7].

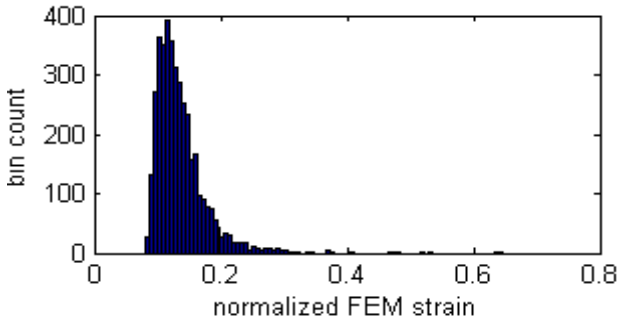

Fig. 7.a. Histogram of the normalized strain in the test dataset.

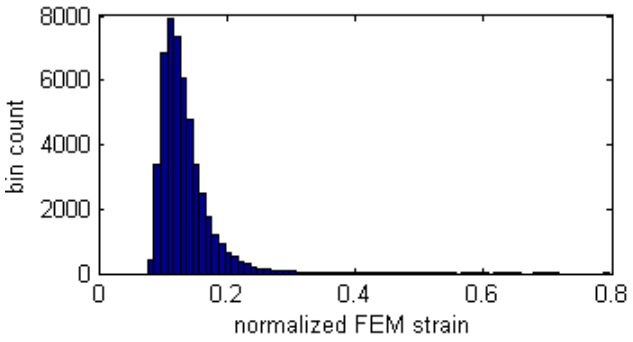

Fig. 7.b. Histogram of the normalized strain in the training dataset.

TABLE 1
Detailed Analysis of Errors

ML method	Bin range	Bin count	Mean relative error (%)	Max relative error (%)	Pearson correlation
CNN	0-0.1	400	3.79	14.85	0.727
	0.1-0.12	1194	4.42	17.85	0.714
	0.12-0.14	1010	5.25	34.58	0.582
	0.14-0.16	622	5.97	36.16	0.433
	0.16-0.18	326	8.26	29.15	0.192
	0.18-1	448	14.08	59.31	0.687
SVM	0-0.1	400	3.36	9.05	0.773
	0.1-0.12	1194	4.05	17.95	0.733
	0.12-0.14	1010	5.76	19.24	0.513
	0.14-0.16	622	7.04	31.66	0.411
	0.16-0.18	326	10.28	33.31	0.221
	0.18-1	448	18.03	64.54	0.578

Since the deep learning algorithm learns the output of a FEA model with almost perfect results, the limitations are mainly given by the limitations of the FEA model. Specifically, the methodology should also be evaluated for nonlinear FEA models, and/or anatomical models with spatially varying mechanical properties (e.g. Young's modulus).

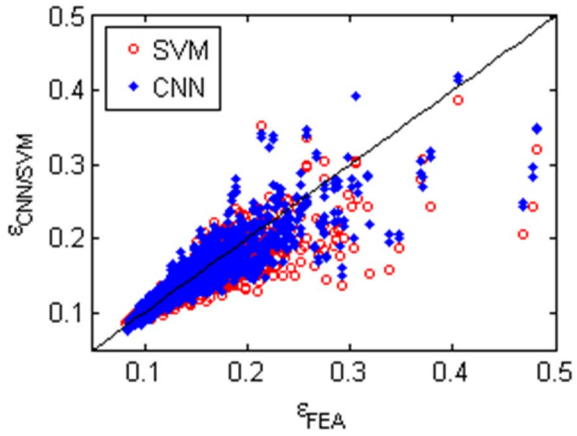

Fig. 8. Scatter plot of strains computed with the CNN/SVM vs. strains computed with the FEA model.

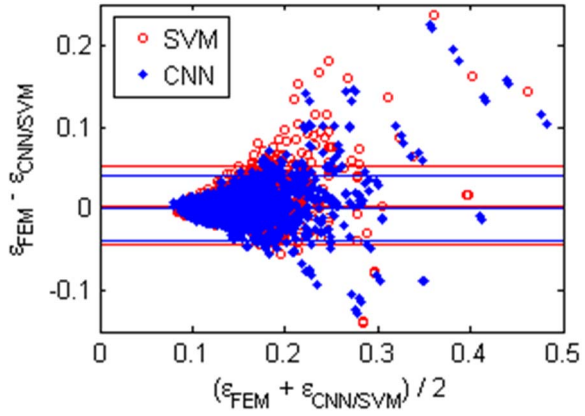

Fig. 9. Bland-Altman analysis of predicted strains (with 95% limits of agreement: ϵ_{CNN} 1.7e-3 ± 0.04; ϵ_{SVM} 4e-3 ± 0.048)

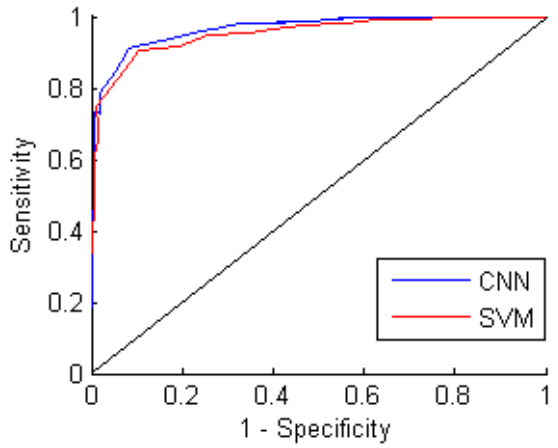

Fig. 10. Receiver-operator characteristic curve. (CNN AUC = 0.968; SVM AUC=0.956)

V. Conclusions

Finite element analyses have proven to be more accurate than the current standardized evaluation method (DXA) for assessing osteoporotic tissue damage.

A method for predicting strains for trabecular tissue structures using a convolutional neural network was presented. The CNN offered a performance increase as against the results obtained with a support vector machine trained on handcrafted features. Deep learning methods speed up the process of patient-specific pathologic assessment by replacing FEA (a resource intensive and time consuming method). The process of synthetic dataset generation and model training is conducted offline, whereas the patient specific predictions are performed online in near real time, being thus well suited for a routine clinical setting.

Future work will focus on validating the proposed method on patient-specific data and developing a methodology for risk score generation based on the predicted measures of interest.

Acknowledgment

This work was supported by a grant of the Romanian National Authority for Scientific Research and Innovation, CCCDI – UEFISCDI, project number ERANET-FLAG - CONVERGENCE (2), within PNCDI III.

References

[1] P. Sambrook and C. Cooper, "Osteoporosis", Lancet, 2006.
[2] J. Kanis and O. Johnell, "Requirements for DXA for the management of osteoporosis in Europe," in *Osteoporosis International,* vol. XVI, 2005, pp. 229-238.
[3] N. Willems, G. Langenbach, V. Everts and A. Zentner, "The microstructural and biomechanical development of the condylar bone: a review" in *European Journal of Orthodontics,* vol. XXXVI, 2014, pp. 479-485.
[4] S. Liew et al., "Method for bone structure prognosis and simulated bone remodeling", US patent no. 20050148860A1, 2004.
[5] A. Zadpoor, G. Campoli and H. Weinans, "Neural network prediction of load from the morphology of trabecular bone" in *Applied Mathematical Modelling,* vol. XXXVII, Elsevier, 2013, pp. 5260-5276.
[6] E. Taghizadeh, M. Kistler, P. Büchler and M. Reyes, "Fast Prediction of Femoral Biomechanics Using Supervised Machine Learning and Statistical Shape Modeling" in *Computational Biomechanics for Medicine,* vol. X, Springer, 2015, pp. 115-127.
[7] C. Ciusdel et al., "Towards Real Time Machine Learning based Estimation of Fracture Risk in Osteoporosis Patients", Proceedings of OPTIM-ACEMP, 2017.
[8] J. Rho and R. Ashman, "Young's modulus of trabecular and cortical bone material: ultrasonic and microtensile measurements" in *Journal of Biomechanics,* 1993.
[9] K.J. Bathe, "Finite element procedures", Prentice Hall, 1996.
[10] A. Speirs and M. Heller, "Physiologically based boundary conditions in finite element modelling", Elsevier, 2006.
[11] Caffe Deep Learning Framework, http://caffe.berkeleyvision.org/.
[12] T. Burgers and J. Mason, "Compressive properties of trabecular bone in the distal femur", Elsevier, 2007.